Diversity-Oriented Synthesis of Functional Polymers with Multisubstituted Small Heterocycles by Facile Stereoselective Multicomponent Polymerizations

Xinnan Wang,[†, ‡] *Ting Han,*[*, §] *Junyi Gong,*[†, ‡] *Parvej Alam,*[†, ‡] *Haoke Zhang,*[±] *Jacky W. Y. Lam,*[*, †, ‡] *Ben Zhong Tang*[*, †, §, ‡, ǁ]

[†]Department of Chemistry, The Hong Kong Branch of Chinese National Engineering Research Center for Tissue Restoration and Reconstruction, and Guangdong-Hong Kong-Marco Joint Laboratory of Optoelectronic and Magnetic Functional Materials,

The Hong Kong University of Science and Technology,

Clear Water Bay, Kowloon, Hong Kong, China

[‡]HKUST-Shenzhen Research Institute, No. 9 Yuexing 1st RD, South Area, Hi-tech Park, Nanshan, Shenzhen 518057, P. R. China

§Center for AIE Research, Shenzhen Key Laboratory of Polymer Science and Technology, Guangdong Research Center for Interfacial Engineering of Functional Materials, College of Materials Science and Engineering, Shenzhen University, Shenzhen 518060, China

±MOE Key Laboratory of Macromolecular Synthesis and Functionalization, Department of Polymer Science and Engineering, Zhejiang University, Xihu District, Hangzhou, 310027 China

ǁShenzhen Institute of Aggregate Science and Technology, School of Science and Engineering, The Chinese University of Hong Kong, Shenzhen, 2001 Longxiang Boulevard, Longgang District, Shenzhen City, Guangdong 518172, China

KEYWORDS: multicomponent polymerization, heterocyclic polymer, aggregation-induced emission

ABSTRACT: Multicomponent polymerization (MCP) has received world-wide attention as a powerful synthetic strategy toward various polymers with complex structures. However, few studies have been reported to fully utilize the monomer combination diversity of MCPs to facilitate the synthesis of diversified polymers with novel structures and advanced functionalities. Herein, we reported a facile multicomponent polymerization route based on the diversity-oriented synthesis. Using varying combinations of difunctionalizable alkynes, sulfonyl azides and Schiff bases, diverse functional polymers with multisubstituted small heterocycles were successfully produced. High stereoselectivity was observed on specific polymeric products. The obtained azetidine-derivative heterocycles exhibit high stability even after treatment with extra HCl and KOH for 48 h. Additionally, polymers with tetraphenylethylene moieties show strong aggregation-induced emission and can function as promising chemosensors for detecting Pd^{2+} and $Cr_2O_7^{2-}$. The facile MCP routes present could bring new inspiration to polymer chemistry, and the fascinating functionalities of the obtained polymers with stable four-membered heterocycles could promote further research on the design, modification, and applications of diversified functional polymer materials.

1. Introduction

It is well-known that subtle difference in microscopic structure can result in dramatically different macroscopic performance.[1] For example, it is the different composition and sequence of base pairs in DNA molecules that contribute to such a complex and diverse biosphere.[2] In materials science, it is of vital importance to design and finely tune the structures at the molecular level to obtain materials with specific functions, and the development of novel polymerization routes is a significant means to achieve such fine tuning of the polymer structures.[3] For example, living free radical polymerization can effectively control the molecular weight of the polymer by adjusting the connection site to obtain the target product with corresponding performance.[4] In the meantime, multicomponent polymerization: with multiple chemical bonds formed in a highly concise fashion, has emerged as a powerful structure tuning strategy.[5]

Multicomponent polymerization (MCP), in which three or more monomers are involved in a one-pot polymeric procedure can be classified as one-step MCP and multi-step MCP.[6] The one-step polymerization enjoys great synthetic simplicity, in which all the monomers and catalysts are added in one-step and reacted within the same period. Representative examples include the one-step Passerini polymerization of aldehyde, carboxylic and isonitrile;[7,8] the A^3-coupling polymerization of alkynes, aldehydes, and amines;[9] the Biginelli polymerization of aryl aldehyde, β-keto ester, and urea (thiourea);[10,11] and the Cu-catalyzed MCP of alkynes, sulfonyl azides with various nucleophiles.[12-16] On the other hand, the multi-step MCP is also known as multicomponent tandem (or cascade) polymerization, in which different monomers and catalysts are added in multi-steps and reacted in a sequential period.[17] Representative examples are Sonogashira polycouplings of alkynes and carbonyl chlorides, followed by a subsequent reaction with nucleophiles such as thiols,[18,19] amines[20,21] , amino ester salts[22] and indoline derivatives.[23] Multicomponent

polymerization integrates numerous advantages such as high efficiency, mild conditions, atom economy and facile construction of complex structure in-situ. A unique and outstanding characteristic of MCP is the product diversity.[24] Firstly, diverse monomers with different structures contribute to versatile products. For example, Choi et al. reported a diversity-oriented polymerization towards 54 samples of graft and dendronized products by polymerizing diverse mono-alkynes, bis-sulfonyl azides and diamines.[12] Secondly, multiple combinations of monofunctional and bifunctional monomers produce polymers with totally different backbone structures. For instance, a three-component polymerization can be theoretically combined in three different ways, namely "$A_2 + B_2 + C_1$", "$A_2 + B_1 + C_2$" and "$A_1 + B_2 + C_2$" (Scheme 1b), potentially affording diverse products with novel structures and functionalities. Few studies have been reported to fully utilize this combination diversity advantage of MCP.

Heterocyclic polymers were first introduced in 1960s to fulfill the requirement of high thermal stability of aerospace materials. They have gradually received consistent academic and industrial interest for their outstanding thermomechanical, dielectric and optical properties.[25] Among various functional polymers, those with small heterocycles such as three- or four-membered heterocyclic polymers are indispensable in organic synthetic chemistry, due to their unique ring-strained structures and distinguished properties such as clusteroluminescence and special stimuli-responsiveness.[26] While our group has widely reported that the preparation of five-membered or six-membered heterocyclic polymers,[19,27-30] those with small heterocycles are rarely studied in our previous work. Firstly, the costly reactants and the difficulty in incorporation of multi-substituents lead to large synthetic challenges. Secondly, the small rings often show low stability where their ring-opening reactions will result in polymer decomposition.[31] Tang et al. reported an in-situ synthesis of 4-membered heterocyclic polymers via multicomponent polymerization.[24] However,

the polymer backbones are vulnerable and easily experience acid hydrolysis. Meanwhile, one of the monomer components in this polymerization cannot be developed into bifunctional molecule, which fails to fully utilize the combination diversity of MCP.

Attracted by the unique properties of polymers with small heterocycles and inspired by the advantages of MCP, we aim to utilize MCP for facile construction of diverse 4-membered heterocyclic polymers. With this purpose, a three-component reaction of alkynes, sulfonyl azides and Schiff bases towards azetidine derivatives has drawn our attention (Scheme 1a).[32] The reaction proceeds efficiently at room temperature with high atom economy in high yields. It is also worth noting that all the third components can be developed into a variety of bifunctional monomers. Based on this reaction, we successfully developed a facile access to functional polymers with multisubstituted four-membered heterocycles. Distinct from the previous work, all the monomers including alkynes, sulfonyl azides and Schiff bases are respectively bifunctionalized, with which all the possible monomer combination ways ("$A_2 + B_2 + C_1$", "$A_2 + B_1 + C_2$" and "$A_1 + B_2 + C_2$") are successfully realized (Scheme 1b). This enables the polymer chain to extend in all possible directions which greatly enhances the product diversity. All polymerizations perform efficiently under mild conditions with good tolerance to different functional groups. The resulting polymers exhibit distinguished properties such as high chemical stability after acid and base treatment, and stereoselectivity was observed on specific polymeric products. Furthermore, they show typical aggregation-induced emission characteristics and can function as a promising fluorescent chemosensor in response to Pd^{2+} and $Cr_2O_7^{2-}$. The feasible and diverse MCP strategy used in this work will provide useful guidance to future research constructing and expanding functionalized small-membered heterocyclic polymers.

Scheme 1. (a) Multicomponent reaction toward *N*-sulfonylazetidin-2-imines. (b) Multicomponent polymerizations toward various azetidine-containing polymers.

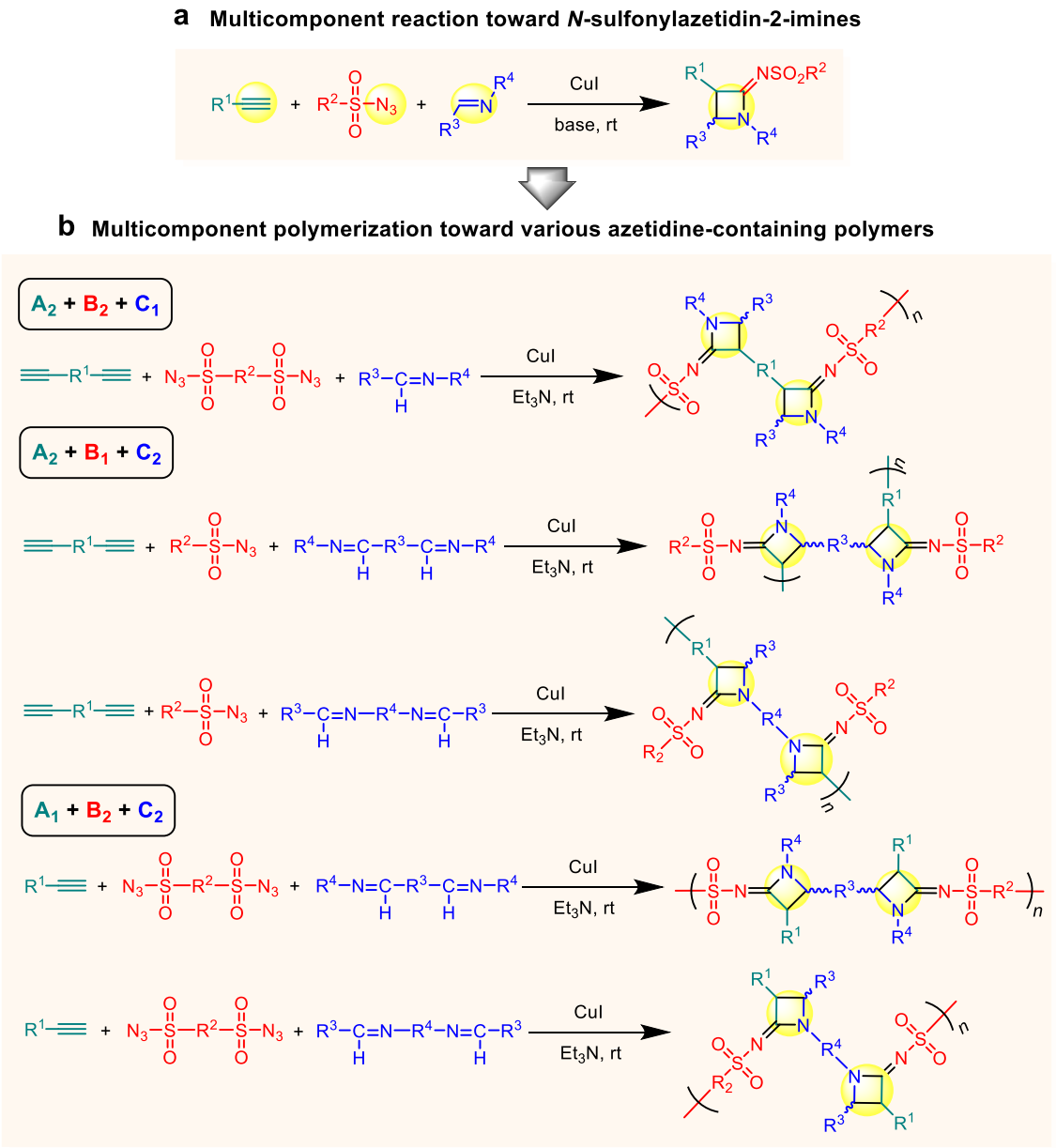

Scheme 2. Multicomponent Polymerization of **1a**, **2a** and **3a**

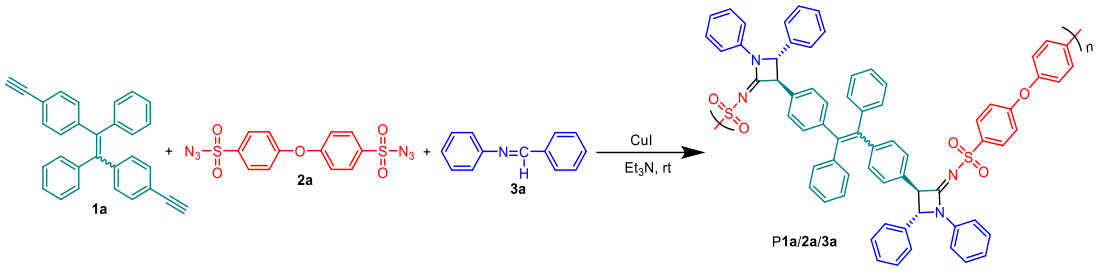

Table 1. Optimizations of Polymerization Conditions of **1a**, **2a** and **3a**[a].

Entry	Base (M)	[**1a**] (M)	Yield (%)	M_n[b]	M_w[b]	PDI[b]
1	Pyridine (0.27)	0.20	61	3700	6600	1.8
2	2,6-Lutidine (0.27)	0.20	66	3700	6200	1.7
3	Et_3N (0)	0.20	Trace	—	—	—
4	Et_3N (0.27)	0.20	62	5300	11500	2.2
5	Et_3N (0.60)	0.20	65	4700	12700	2.7
6	Et_3N (0.40)	0.20	68	5600	13600	2.4
7	Et_3N (0.80)	0.20	Gel	—	—	—
8	Et_3N (0.27)	0.10	51	3400	6600	1.9
9	Et_3N (0.27)	0.25	62	4700	11100	2.4
10	Et_3N (0.27)	0.30	60	4800	10700	2.2
11[c]	Et_3N (0.27)	0.40	Gel	3400	7900	2.3

[a] Carried out at room temperature under nitrogen in dichloromethane for 12 h, [**2a**] = [**1a**], [**3a**] = 2.4 [**1a**], [CuI] = 20 mol%. [b] Estimated by GPC in THF on the basis of a linear polystyrene calibration. PDI = M_w/M_n. [c] The GPC result is for the soluble fraction.

2. Results and Discussion

Polymerization

All the monomers used in this work are easily accessible. The diyne **1a**, disulfonyl azide **2a-d** and Schiff base **3b-e** were respectively prepared following the literature procedures.[33,34] All the polymerizations proceeded in one-pot in the presence of triethylamine (Et_3N) and copper iodide (CuI) at ambient temperature under nitrogen atmosphere. The impacts of reaction parameters including the solvent, catalyst, base, and monomer concentration were systematically investigated, which aimed at generating soluble polymers with high molecular weights in high yields.

Taking the polymerization of **1a**, **2a** and **3a** as an example (Scheme 1), the effect of solvent was first examined (Table S1, entry 1-5). Among all the tested organic solvents, the polymerization in dichloromethane (DCM) afforded the polymer with the highest molecular weight (M_w = 11500) in a relatively high yield of 62%. Regarding the catalyst loading (Table S1, entry 5-6), the use of the copper oxide (Cu_2O) led to a dramatic decrease in both yield and molecular weight, thus CuI was chosen as the preferred catalyst. Next, the base effect on the polymerization (Table 1, entry 1-7) was examined, which plays a crucial part as the small molecule synthesis reported in the literature.[32] The common organic bases including pyridine, 2,6-lutidine and Et_3N all gave the desired polymeric products with expected structures, among which Et_3N afforded the polymer with the highest molecular weight (M_w) of 11500. The effect of Et_3N concentration on the polymerization was then examined (Table 1, entry 3-7). The polymerization failed to proceed without the addition of base. On the other hand, the increase of the base concentration from 0.27 M to 0.6 M exerted little influence on the yield and molecular weight. Further elevation of the concentration to 0.8 M led to the gel formation. Considering the economy and polymer solubility, 0.27 M was adopted as the optimal base concentration. To further increase the polymerization

efficiency, the effect of monomer concentration was then evaluated and summarized in Table 1, Entry 4, 8-11. Keeping [**1a**]:[**2a**]:[**3a**] = 1:1:2.4, a polymer with the highest yield and molecular weight was generated at [**1a**] of 0.2 M. Yet little impact on the polymerization result was observed at a concentration range from 0.2 M to 0.3 M. Further increasing [**1a**] to 0.4 M led to the formation of gelled polymer, in which a noticeable decrease in solubility was observed. Thus, taking the economy, yield and molecular weight into account, 0.2 M of [**1a**] was finally chosen as the optimal monomer concentration.

Scheme 3. (a) Multicomponent polymerization ($A_2 + B_2 + C_1$) of **1a**, **2a-d** and **3a-e**. (b) Chemical structure and polymerization results of P**1a**/**2a-d**/**3a-e**. M_ws are determined by GPC in THF on the basis of a polystyrene standard. TPE represents tetraphenylethylene unit of **1a**.

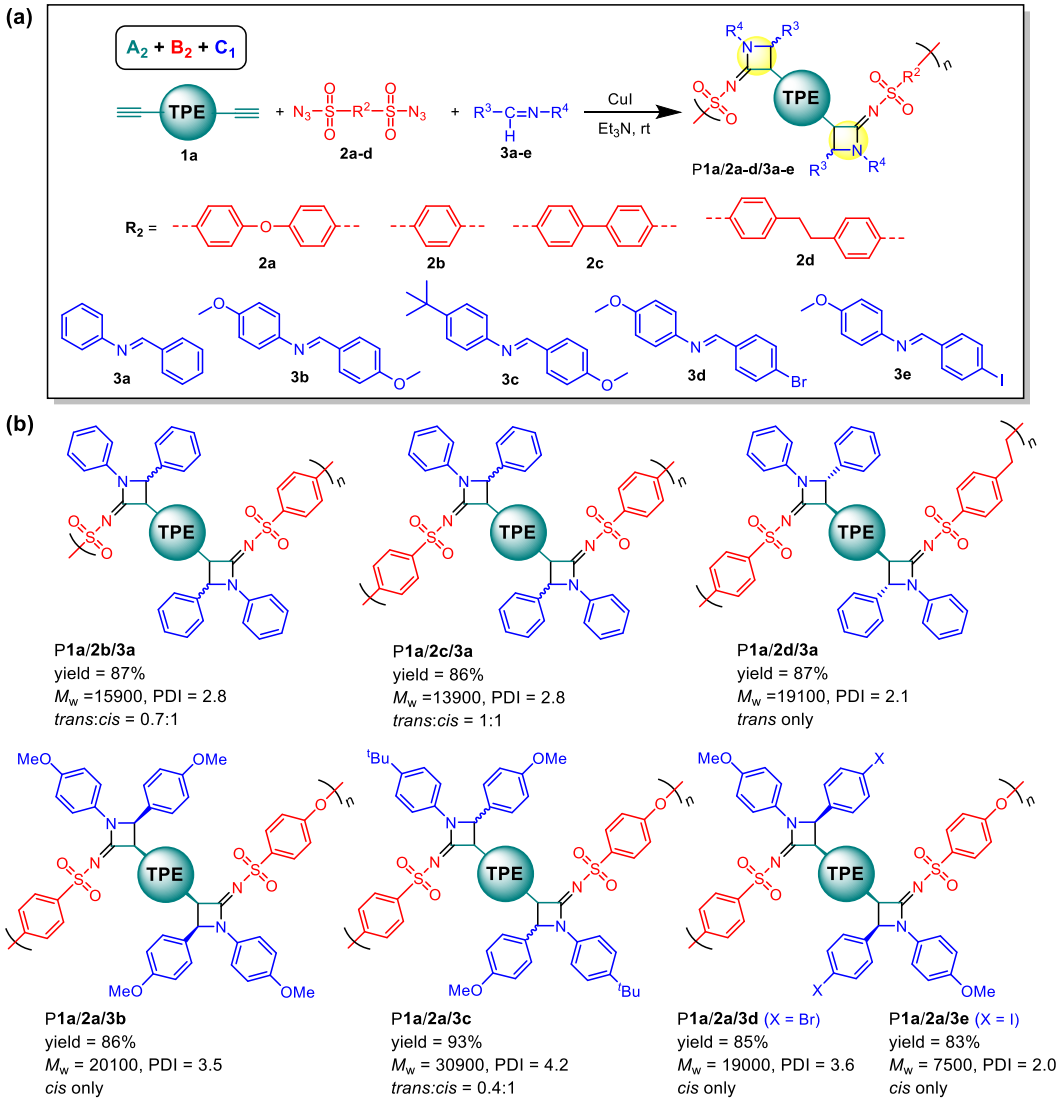

Scheme 4. (a and b) Multicomponent polymerizations in the monomer combination type of "$A_2 + B_1 + C_2$". (c-e) Multicomponent polymerizations in the monomer combination type of "$A_1 + B_2 + C_2$". M_ws are determined by GPC in THF on the basis of a polystyrene standard.

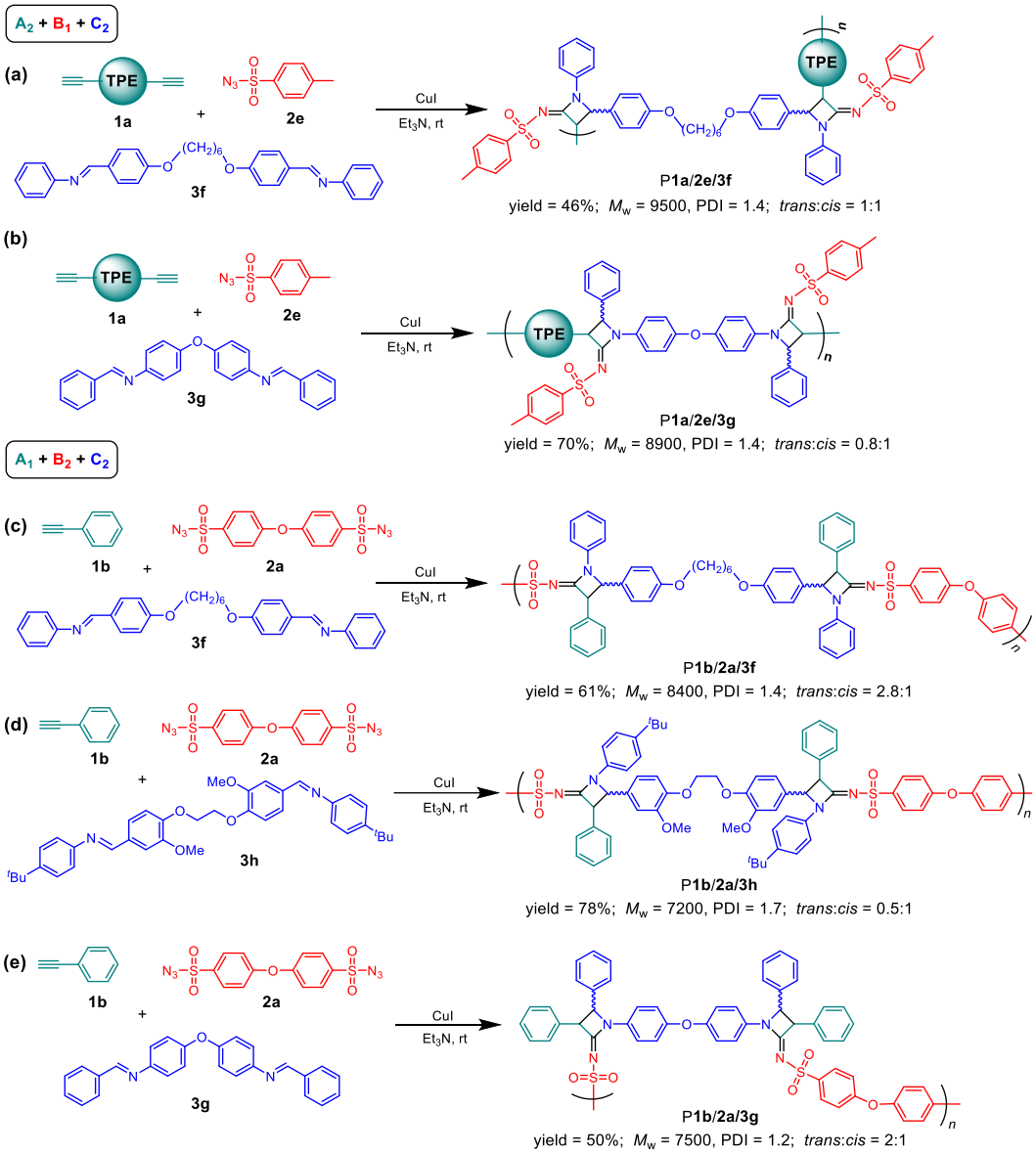

Based on the optimized conditions, we then expanded the monomer scope of the polymerization in the combination mode of "A2 + B2 + C1" first to enrich the structural diversity (Scheme 3a). Various disulfonyl azides and Schiff bases were utilized in the polymerizations with the TPE-containing diyne to generate polymers in good yields of up to 93% and high M_ws of up to 19100 (Scheme 3b). Sulfonyl azide **2b** and **2c** with a rigid structure were also applicable for the polymerization, generating products with M_ws up to 15900 in good yields. When monomer **2d** carrying a flexible alkyl chain was used, the resulting polymer P**1a**/**2d**/**3a** was generated in a high yield of 87% with high molecular weight of 19100. Regarding the monomer scope of Schiff bases, monomer **3b** bearing terminal electro-donating groups was efficient for the polymerization affording the expected polymeric product in a high yield of 86%. Monomer **3c** carrying a bulky *tert*-butyl group was also applicable and effective for the polymerization, yielding a product with a M_w of 30900 in a high yield of 93%. When Schiff base **3d** carrying a halogen atom (Br**)** was employed, the desired polymer was obtained with a M_w of 19000 in a good yield. However, monomer **3e** carrying an iodine atom generated a polymer P**1a**/**2a**/**3e** with a decreased M_w due to its poorer solubility. Inspired by the success in expanding the monomer scope in the combination mode of "$A_2 + B_2 + C_1$", we then explored the expanding possibility of other two combinations modes, "$A_2 + B_1 + C_2$" and "$A_1 + B_2 + C_2$" (Scheme 4). Delightfully, all polymerizations generated the expected azetidine derivative rings along the polymer backbones. However, compared with the forementioned combination mode "$A_2 + B_2 + C_1$", these two combination modes give polymers in lower yield and molecular weights. Some unidentified structures were also found in P**1b**/**2a**/**3f** and P**1b**/**2a**/**3h**. These results can be explained as follows: (1) the decreased solubility of bifunctional Schiff bases decreases the efficiency of the polymerization; (2) according to the mechanism reported by previous literature,[32] these reactions follow the pathway that the alkyne group first

reacts with sulfonyl azide to form an intermediate, which further reacts with the imine bonds of Schiff base to yield the 4-membered heterocycles. The two monomer combination modes ("A_2 + B_1 + C_2" and "A_1 + B_2 + C_2") shown in Scheme 4 suffer relatively higher steric hindrance that is detrimental to the chain propagation of the polymerizations. Yet they are still effective means to broaden the polymerization applicability. The results shown in Scheme 3 and 4 together demonstrate that this MCP tool has a great tolerance to different functional groups, and has fully utilized the monomer diversity and combination diversity to provide a facile access to diverse polymers with multisubstituted small heterocycles.

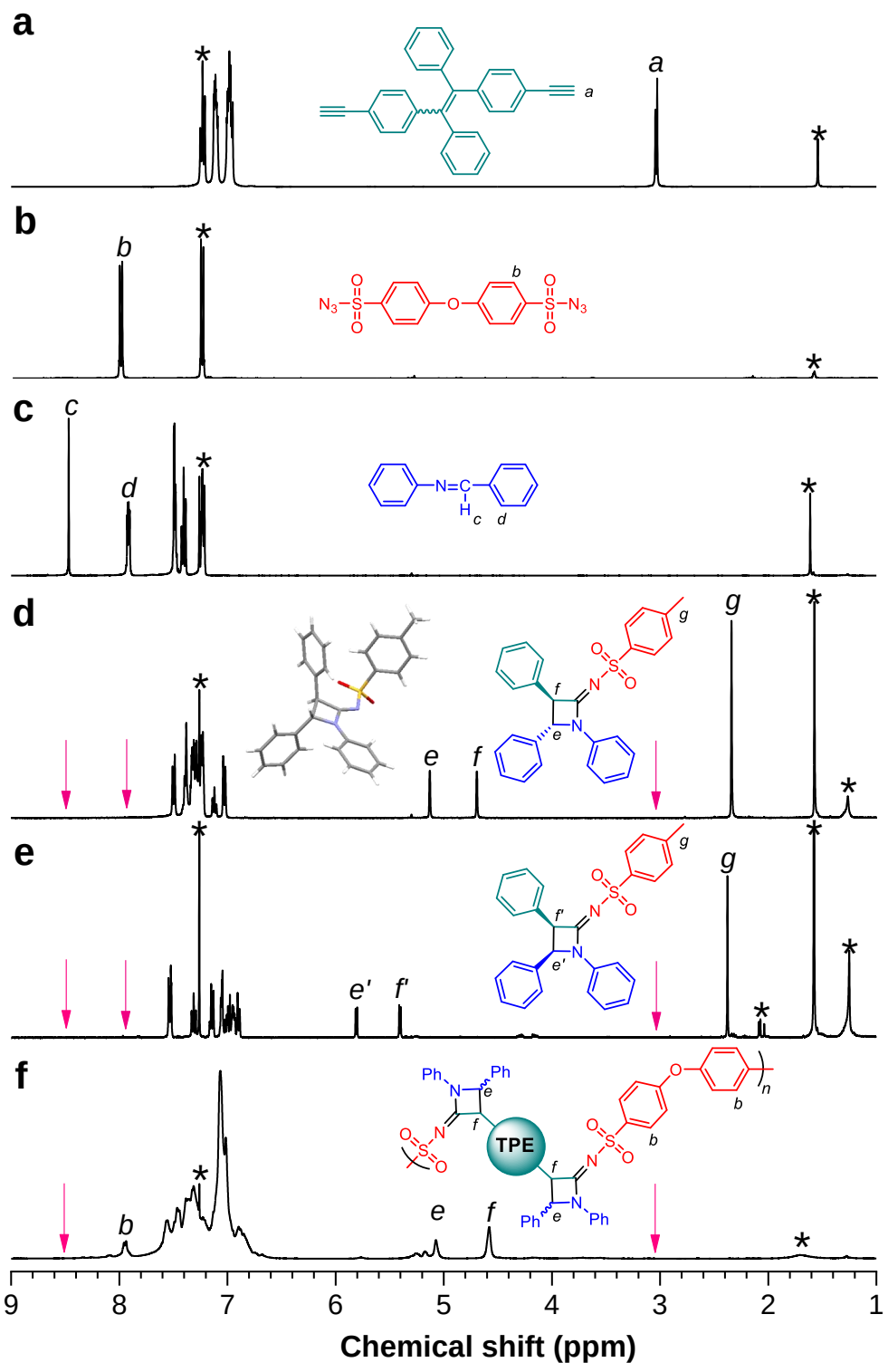

Figure 1. ^{1}H NMR spectra of (a) **1a**, (b) **2a**, (c) **3a**, (d) *trans*-**M** and (e) *cis*-M and (f) P**1a/2a/3a** in chloroform-*d*. The solvent peaks are marked with asterisks.

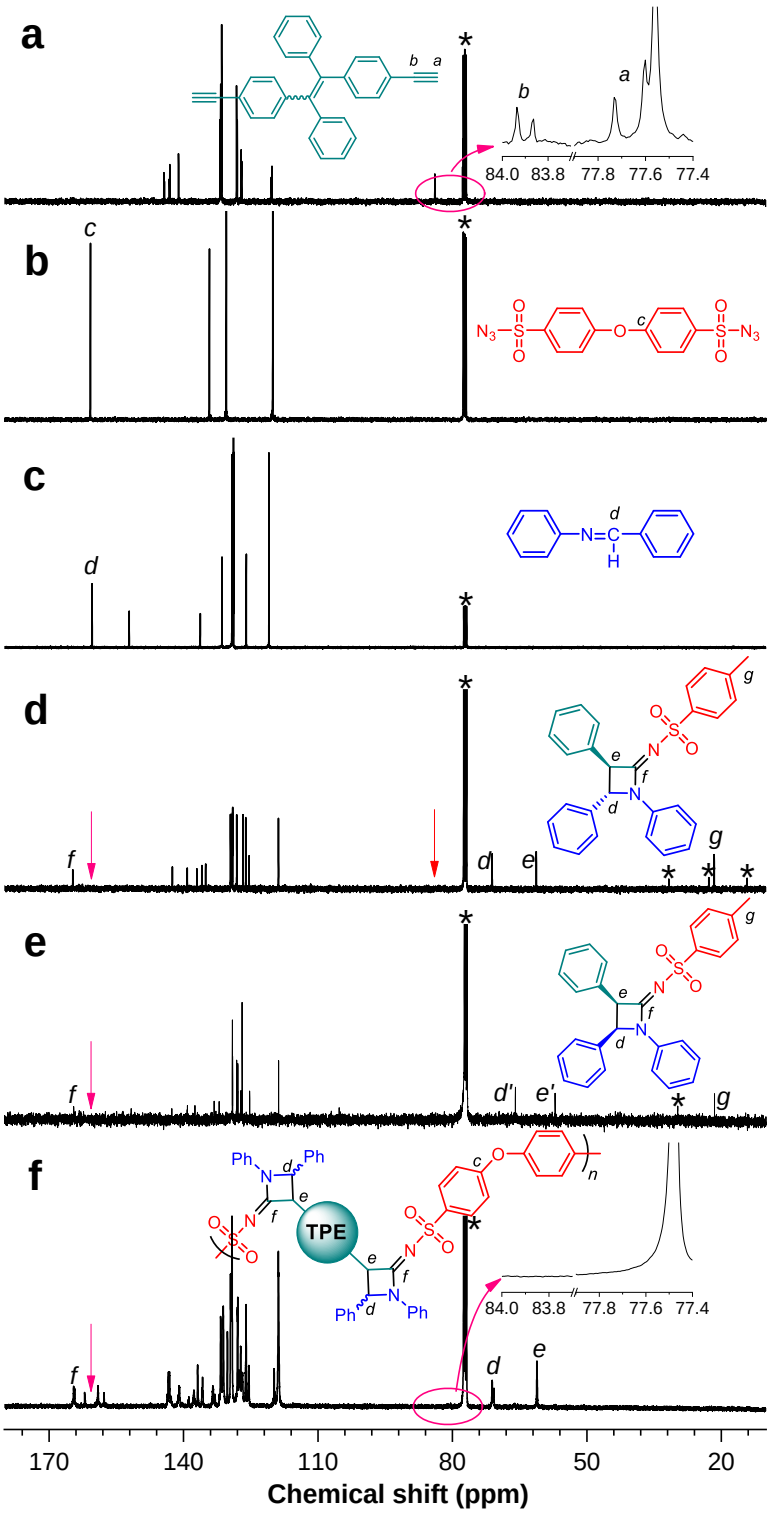

Figure 2. ^{13}C NMR spectra of (a) **1a**, (b) **2a**, (c) **3a**, (d) *trans*-**M** and (e) *cis*-M and (f) P**1a/2a/3a** in chloroform-*d*. The solvent peaks are marked with asterisks.

3. Structural Characterization

To get an insight into the structures of the obtained polymers, a model compound was synthesized from phenylacetylene, 4-methylbenzenesulfonyl azide and *N*-benzylideneaniline. Consistent with the reported literature,[32] it was found that both cis (*cis*-**M)** and trans (*trans*-**M)** isomers were produced and their structures were fully characterized by high-resolution mass spectrometry (Figure S1 and S2), IR specctroscopy (Figure S3), NMR techniques (Figure 1 and 2) and single crystal X-ray diffraction (Figure 1d and Table S2). The structures of all the obtained polymers were also confirmed by the above-mentioned methods.

The characterization results of P**1a**/**2a**/**3a** were compared with the model compounds (*trans*-**M** and *cis*-**M)** and the corresponding monomers, which was discussed as an example. As shown in the IR spectrum provided in Figure S3, the ≡C-H and C≡C stretching vibration of **1a** were observed at 3271 and 2104 cm^{-1} respectively, while the stretching vibration bands of N_3 of monomer **2a** were found at 2128 and 2160 cm^{-1}. All these characteristic peaks disappeared in both the model compounds and P**1a**/**2a**/**3a**, suggesting the complete consumption of C≡C and N_3 groups during the polymerization.

^{1}H NMR analysis was conducted to obtain more detailed information of the polymer structure. As shown in Figure 1, the acetylene proton of **1a** resonated at δ 3.03, which disappeared in both model compounds and P**1a**/**2a**/**3a**. The resonance peak in "d" position of monomer **3a** at δ 7.92 shifted to the broad peak in aromatic zone in the spectrum of P**1a**/**2a**/**3a**. The peak in "c" position at δ 8.47 shifted to δ 5.07 with the formation of a new peak at δ 4.58 in the spectrum of P**1a**/**2a**/**3a**. Compared with *trans*-**M**, these two peaks can be respectively assigned as the protons of P**1a**/**2a**/**3a** in "e" and "f" position, suggesting the formation of the 4-membered heterocycle. ^{13}C NMR analysis was conducted to further verify the polymer structure (Figure 2). The resonance bands of

acetylene carbons of monomer **1a** were located at δ 83.93 and δ 77.73 respectively, which were not found in the model compounds and P**1a**/**2a**/**3a**. This suggested the fully conversion of the C≡C.[35] The resonance signal at δ 160.49 in "d" position of monomer **3a** shifted to δ 71.05 in the polymer. Meanwhile, two new peaks at δ 61.14 and δ 164.41 were observed. These two peaks were associated with the carbon atoms in newly formed 4-membered heterocycle with a trans conformation in P**1a**/**2a**/**3a**, which were consistent with the chemical shift of those in *trans*-**M**. All these results confirmed the formation of target polymer with a precise structure as shown in Scheme 3a.

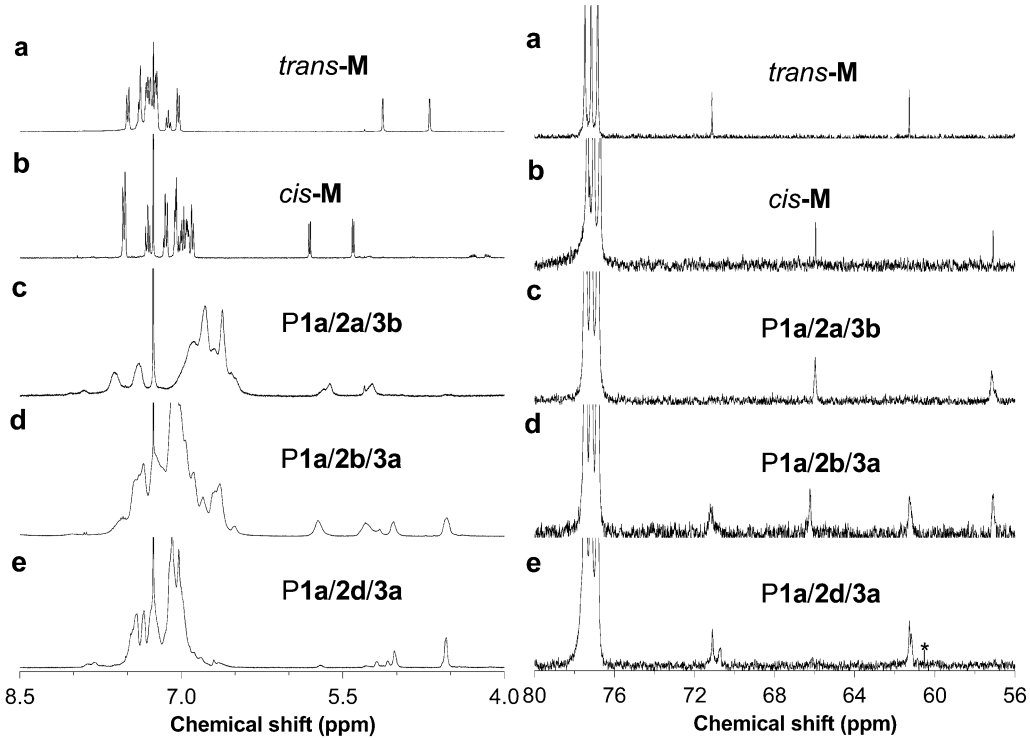

Figure 3. Comparison of the characteristic peaks of the four-membered ring in the ^{1}H NMR spectra (left) and ^{13}C NMR spectra (right) of (a) *trans*-**M**, (b) *cis*-**M**, (c) P**1a**/**2a**/**3b**, (d) P**1a**/**2b**/**3a**, (e) P**1a**/**2d**/**3a** in chloroform-*d*. The solvent peaks were marked with asterisks.

As previously described, stereoisomerisms were generated during the model reaction, which is consistent with the reported literature.[32] The configuration of the trans model compound (*trans*-**M**) was verified by the single crystal X-ray diffraction (Figure 1d and Table S2). Analysis by ^{1}H NMR showed that the resonance bands of the two protons of the heterocycle of *trans*-**M** were located at δ 5.13 and δ 4.69 respectively. The corresponding proton resonances of *cis*-**M** were found at δ 5.80 and δ 5.39 (Figure 3a-b, left column). The ^{13}C-NMR analysis showed the consistent results. The resonance bands of the two tertiary carbons in the heterocycle of *trans*-**M** at δ 71.14 and δ 61.28 shifted to δ 65.94 and δ 57.09 in *cis*-**M** (Figure 3a-b, right column), respectively. This chemical shift can be used to identify the stereoisomerism in polymeric products, and the integrals of these characteristic resonance peaks in the ^{1}H-NMR spectra help us determine the corresponding ratio of the *trans* and *cis* configuration. There are totally three situations: (1) only *cis* configuration is produced such as the heterocycles in P**1a**/**2a**/**3b** (characteristic peaks shown in Figure 3c); (2) both *trans* and *cis* configurations are produced such as those in P**1a**/**2b**/**3a** (Figure 3d); (3) only trans configuration is produced such as those in P**1a**/**2d**/**3a** (Figure 3e)**.** The stereoselectivity occurs in case (1) and (3) and are all repeatable. The stereoselectivity of all the polymers are labelled in Scheme 3b and Scheme 4. The factors contributing to stereoselectivity are complex and may work collectively, such as the steric hindrance, electron density and tension force of the small heterocycle.[36] As shown in Scheme 3b, all the stereoselective polymerization (P**1a**/**2d**/**3a**, P**1a**/**2a**/**3b**, P**1a**/**2a**/**3d** and P**1a**/**2a**/**3e)** in the monomer combination mode "$A_2 + B_2 + C_1$" shared a common characteristic: all of them used sulfonyl azide with a flexible chain (**2a** or **2d**). When this monomer was replaced with a rigid chain (**2b** or **2c**), the regioselectivity in the resulting polymers P**1a**/**2b**/**3a** and P**1a**/**2c**/**3a** became poorer. Only one exception was observed in P**1a**/**2a**/**3c**, which used flexible azide as monomer however showed no regioselectivity. Also, the regioselectivity is

not observed in polymers prepared by using monomer combination modes of "$A_2 + B_1 + C_2$" and "$A_1 + B_2 + C_2$". The exact reason for this phenomenon remains unclear at present and will be explored in the near future work.

Stability and Solubility

Thermogravimetric analysis (TGA) and differential scanning calorimetry (DSC) measurement were conducted to investigate the thermal and morphological stability of the obtained polymers. Figure S7 illustrates the thermal degradation process of the polymers after heating at a rate of 10 °C/min. All the polymers lost 5% of their weight at 181-268 °C. No glass transition temperatures were detected in their DSC thermograms (Figure S8), possibly ascribed to their rigid structures.[37] All the polymers possessed fairly good solubility, and can be dissolved in common organic solvents, such as dichloromethane, chloroform, dimethyl sulfoxide, and tetrahydrofuran.

Table 2. The condensed Fukui function and condensed dual descriptor (CDD) of nitrogen atoms in **M1**[c] and **M2**.

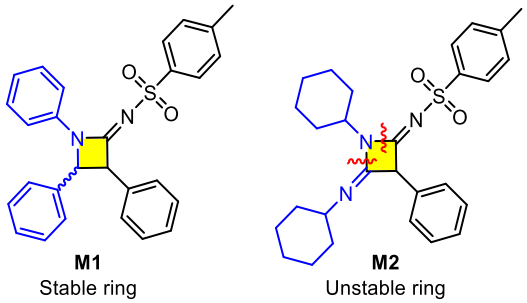

Compound	f^{+} [a]	f^{-} [b]	f^{0} [c]	CDD
M 1	0.0338	0.0670	0.0504	-0.0332
M 2	0.0434	0.0855	0.0644	-0.0421

[a] f^{+} function represents the initial parameter of a nucleophilic reaction. [b] f^{-} function represents the initial parameter of an electrophilic reaction. [c] **M1** is stable under the tested conditions: 25 equiv. HCl in water/THF mixture under stirring for 48 h; 25 equiv. KOH in water/THF mixture under stirring for 48 h.

We then tested the chemical stability of the polymers under acidic and basic conditions. It is well-known that the 4-membered heterocycles are vulnerable under extreme pH environment, undergoing ring-opening reactions.[38] To our surprise, both the model compounds and P**1a**/**2a**/**3a** showed no structure change after stirring in excess amount of HCl (25 equiv.) and KOH (25 equiv.) in water/THF mixture for 48 h. Notably, there is a distinctive reactivity difference of the heterocycle obtained in this work compared with the 4-membered azetidine structure we reported before,[24] which experienced a fast acid-mediated ring-opening reaction. To get an insight into this structure-reactivity relationship, DFT calculations on the model compounds of these two works were conducted following the reported literatures.[39-44] The results of the calculated condensed Fukui function and condensed dual descriptor (CDD) of **M1** (stable ring, this work) and **M2** (unstable ring, previous work) were summarized in Table 2. From the condensed Fukui function, the f^- of **M2** (0.0855) was distinctively larger than that of **M1 (**0.0670), indicating the larger electron density of the 4-membered ring in **M2** to experience acidic ring-opening reaction. The same conclusion can be drawn from the calculated condensed dual descriptor (CDD). The CDD of **M2** (-0.0421) was smaller than that of **M1** (-0.0332) which demonstrated the less nucleophilicity of the latter one. The cause of the electron density difference can be further understood by the analysis of the molecular structure. In **M2**, the nitrogen atom of the 4-membered ring is sp^3 hybridized. Thus, the lone pair electrons possessed higher electron density to give rise to stronger nucleophilicity. In **M1**, the nitrogen atom is conjugated with aromatic substituent and is sp^2 hybridized, thus with lower electron density in the heterocycle showing lower nucleophilicity. Herein, the experimental data, theoretical calculation and structure analysis are in perfect agreement. To conclude, the stability difference is attributed to the electron density difference of the 4-membered heterocycle, resulting from the different substituents on the heterocycle. Such

investigation can serve as a useful strategy to optimize the small ring stability by adjusting the ring electron density.

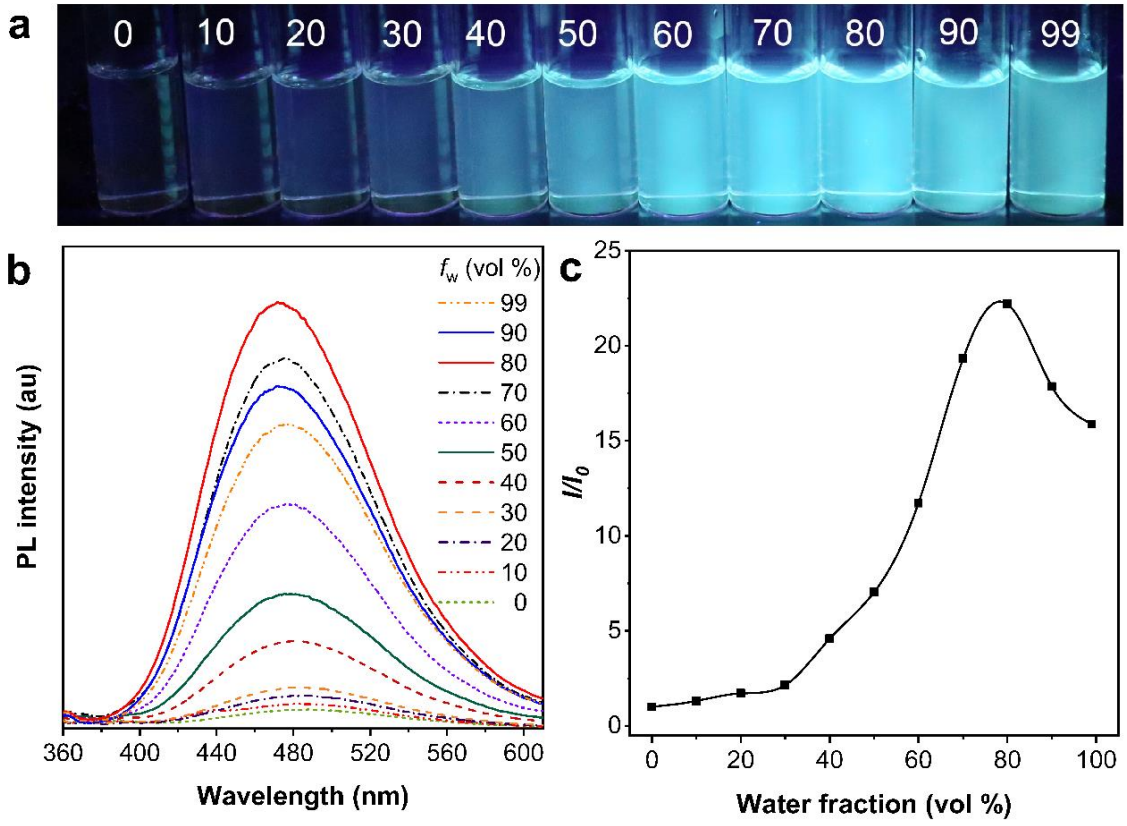

Figure 4. (a) Photographs of P**1a**/**2a**/**3a** in THF/water mixtures with different water fractions (f_w) taken under 365 nm UV irradiation from a hand-held UV lamp. (b) Photoluminescence (PL) spectra of P**1a**/**2a**/**3a** in THF/water mixtures with different water fractions (f_w). Excitation wavelength: 330 nm. (c) Photographs and plot of the relative emission intensity (I/I_0) versus the composition of the THF/water mixture of P**1a**/**2a**/**3a**. Solution concentration: 10 μM.

Photophysical Properties

Aggregation formation is a well-known natural process causing fluorescence quenching in traditional fluorophores, which therefore became a stumbling block for their practical applications.[45] Our group firstly reported an opposite phenomenon in 2001 called aggregation-induced emission (AIE). AIE luminogens are faintly emissive in solutions but show intense emission enhancement upon aggregation formation.[46] Since TPE is a representative AIE-active moiety,[47] the polymers obtained in this work are anticipated to be AIE-active. Thus, their photophysical properties are systematically investigated.

The absorption spectra of the polymers in dilute (10^{-5} M) THF solutions were shown in Figure S9. All the spectra were peaked at similar wavelengths (~330 nm). Then their photoluminescence (PL) in THF/water mixtures with different water fractions (f_w) was studied. The PL spectra of P**1a**/**2a**/**3a** are given in Figure 4 as an example. When f_w was lower than 40%, no obvious emission was observed. Afterwards, a noticeable signal was detected due to the aggregate formation. The PL intensity kept rising upon addition of more water and reached its maximum at the f_w of 80% at 475 nm, which was 22-fold higher than that in pure THF solution (Figure 4B). The PL intensity then slightly decreased with the further addition of water. This is commonly observed in PL spectra of AIE polymers due to the formation of large-sized aggregate at high water content, which decrease the effective concentration of polymer mixtures.[48] The PL behavior of P**1a**/**2a**/**3a** in THF/water mixtures with different f_w could be directly visualized. Together with the PL spectra of other TPE-bearing polymers (Figure S10), it clearly demonstrated the AIE feature of the obtained polymers. The active intramolecular motions of the TPE unit is restricted in the aggregate state, which blocks the nonradiative decay pathway of the excited state to enable the polymers to show intense emission.[49]

Ion Detection

Palladium and chromium are common heavy metal elements with potential health hazards. Palladium, which is widely used as the catalyst in organic synthesis, its divalent residue in low dose is sufficient to cause deterioration in optoelectronic devices or allergic reactions in susceptible individuals.[17,50] Chromium, especially in its hexavalent state (Cr (VI)), is carcinogen with strong oxidizing ability, exposure to which leads to not only potential irritation, but the risk of severe mutagenic and cell damage.[51] To make matters even worse, these heavy metals can move up the food chain in progressively greater concentrations by biological magnification.[52] The detection of divalent palladium and hexavalent chromium are therefore of vital importance. As P**1a**/**2a**/**3a** is an AIE macromolecule with merits of high reliability, sensitivity, and selectivity,[53] we investigated its potential application in ion detection. To our surprise, it exhibits good response as a bifunctional probe towards the detection of these two ions.

The PL spectra of P**1a**/**2a**/**3a** (10 μM) in 80% aqueous mixtures (f_w = 80%) with different concentrations of palladium ion (Pd^{2+}) were shown in Figure 5a. By increasing the Pd^{2+} concentration from 0 to 0.84 mM, the spectra profile remained unchanged, but a distinct and progressive PL intensity decrease was observed. More details on the quenching process were provided in the Stern-Volmer plot shown in Figure 5b.[54] The quenching constants calculated from the linear region increased sequentially from 8330 M^{-1} to 24150 M^{-1} and then 107140 M^{-1}, showing a super amplification quenching effect.[55] The limit of detection (LOD) was calculated according to the equation LOD = 3SB/m (SB = the standard deviation of the repeated 8 blank measurements, and m = the slope of the relative intensity over Pd^{2+} concentration), and was equal to 8.5×10^{-6} M, indicative of good sensitivity.[56] Then the selectivity of P**1a**/**2a**/**3a** as Pd^{2+} sensor was investigated. By comparing the relative PL intensity of P**1a**/**2a**/**3a** with the presence of 16 common metal cations

including Pd^{2+}, Fe^{3+}, Co^{2+}, Ca^{2+}, Al^{3+}, Cr^{3+}. Cu^{2+}. Pb^{2+}. Zn^{2+}, K^{+}, Cd^{2+}, Mg^{2+}, Na^{+}, Mn^{2+}, Ag^{+}, and Sn^{2+} under the same condition, it was found that the polymer showed distinctly stronger quenching response to Pd^{2+}, which indicated its good selectivity as metal cationic probe to Pd^{2+} (Figure 5c).

P**1a**/**2a**/**3a** also served as a potential bifunctional anion probe. As shown in Figure 5d, a PL quenching response was observed upon addition of potassium dichromate to its 80% aqueous mixture. A similar quenching amplification effect was found, where the quenching constants raised from 3390 M^{-1} (0-0.2 mM $K_2Cr_2O_7$ solution) to 12140 M^{-1} (0.2-0.6 mM $K_2Cr_2O_7$ solution) and then to 36210 M^{-1} (0.6-0.8 mM $K_2Cr_2O_7$ solution). The LOD of Cr (VI) was calculated to be 2.09×10^{-5} M and the polymer again exhibited superior selectivity to it among 11 common anions (Figure 5f).

Considering applications in daily life, the in-situ detection working on the solid support requires no sophisticated equipment, with higher efficiency and lower cost than the "wet" detection.[57,58] In view of this, we tested whether this bifunctional ion probe can be applied in the solid state. By dipping a thin layer chromatography (TLC) plate into P**1a**/**2a**/**3a** solution, the polymer was coated onto the plate and showed bright emission under portable 365 nm UV flashlight (Figure 5g). Then Pd^{2+} (Figure 5h) and $Cr_2O_7^{2-}$ solution (Figure 5i) were respectively spotted on plates using a capillary tube, giving quenching circle of ~0.4 cm^2 under UV light. This quenching phenomenon can be clearly visualized by naked eyes to identify the tested ion. Another "solid" measurement was performed by adsorbing P**1a**/**2a**/**3a** onto a filter paper. $Cr_2O_7^{2-}$ solution was then used as "ink" to draw on the filter paper by a glass tube. A "Swan" graph could be clearly identified under UV light owing to the quenching effect (Figure 5j). The same operation worked successfully when replacing "$Cr_2O_7^{2-}$" with Pd^{2+}. Both experiments demonstrated the high feasibility of using AIE-active P**1a**/**2a**/**3a** as bifunctional probe for daily detection.

We then investigated the quenching mechanism for this AIE ion probe. Due to the absorption similarity of the $Cr_2O_7^{2-}$ and Pd^{2+}, we compared their electronic transitions with other common metal ion, especially chromogenic ions such as Fe^{3+}, Co^{2+}, Cr^{3+} and Cu^{2+}. As shown in Figure S11, the molar absorptivity of Pd^{2+}, $Cr_2O_7^{2-}$ and Fe^{3+} ions were higher than other tested ions. Meanwhile the absorption of $Cr_2O_7^{2-}$ and Pd^{2+} was largely overlapped with the PL spectra of P**1a**/**2a**/**3a** (within 410-530 nm and 410-620 nm), which led to the energy transfer from the excited state of P**1a**/**2a**/**3a** to the ground state of these two ions to result in the emission quenching.[59] It is worth noting that the absorption spectrum of Fe^{3+} also overlaps with the PL spectrum of the polymer but in a much smaller extent, and the Fe^{3+} solution has less molar absorptivity within this wavelength range. This led to the less efficient energy transfer and much weaker PL quenching.

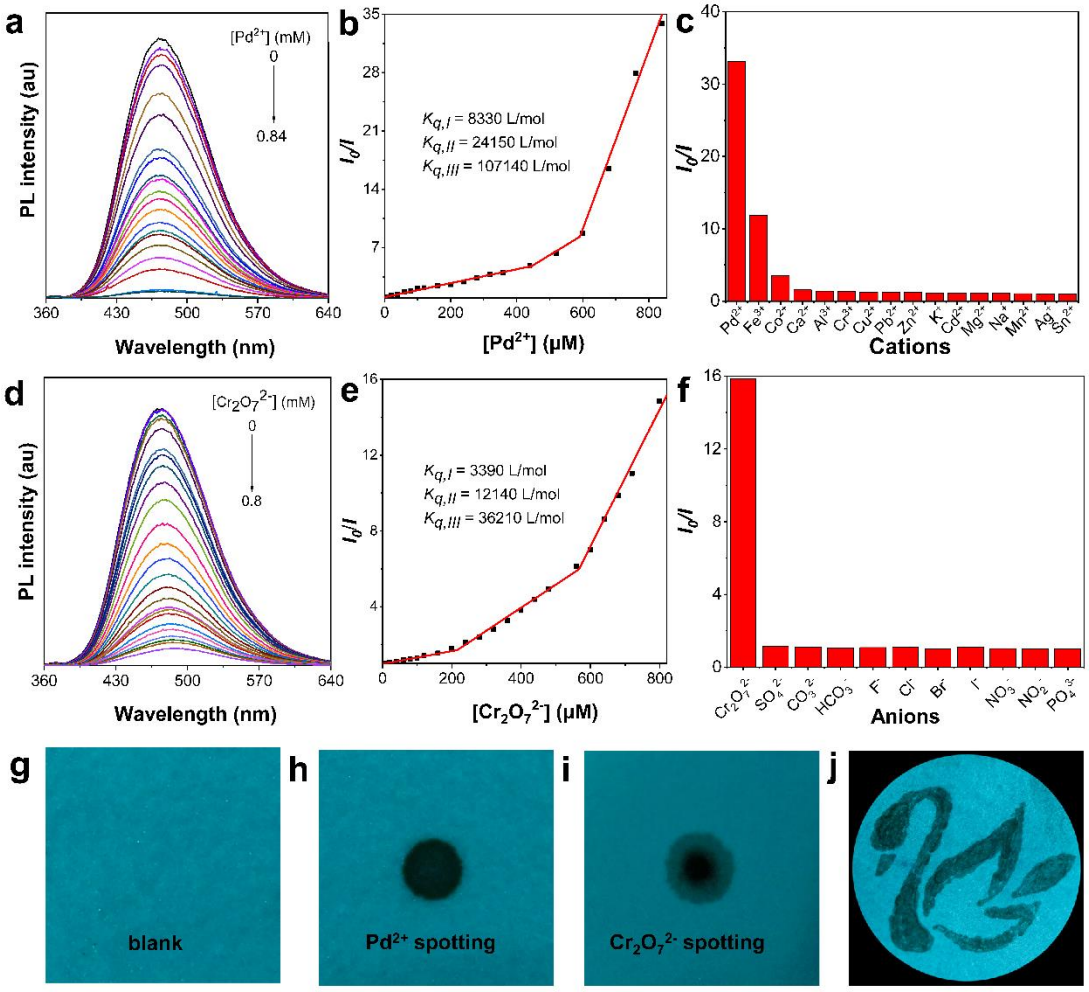

Figure 5. (a) PL spectra of P**1a**/**2a**/**3a** in THF/H_2O mixtures (f_w = 80%, 10 μM) containing different amounts of Pd^{2+}. (b) Stern-Volmer plots of relative intensity (I_0/I) versus the Pd^{2+} concentration. I_0 = PL intensity in the absence of Pd^{2+}. (c) Selectivity of P**1a**/**2a**/**3a** to different metal cations (0.8 mM) in THF/H_2O mixtures (f_w = 80%, 10 μM). I_0 = intensity in the absence of metal cations. (d) PL spectra of P**1a**/**2a**/**3a** in THF/H_2O mixtures (f_w = 80%, 10μM) containing different amounts of $Cr_2O_7^{2-}$. (e) Stern-Volmer plots of relative intensity (I_0/I) versus the $Cr_2O_7^{2-}$ concentration. I_0 = PL intensity in the absence of $Cr_2O_7^{2-}$. (f) Selectivity of P**1a**/**2a**/**3a** to different metal anions (0.8 mM) in THF/H_2O mixtures (f_w = 80%, 10 μM). I_0 = intensity in the absence of metal anions. (g) Fluorescent photographs of P**1a**/**2a**/**3a** deposited on TLC plates, before and after

spotting with (h) Pd^{2+} solutions and (i) $Cr_2O_7^{2-}$ solutions respectively. (j) The image of the "Swan" was drawn on a filter paper by a glass tube using the $Cr_2O_7^{2-}$ solution as the "ink".

4. Conclusions

In this work, we developed a facile access to diverse functional polymers with multisubstituted small heterocycles by multicomponent polymerizations. This strategy enjoys the advantages of readily available monomers, mild conditions, outstanding efficiency, and good tolerance to different functional groups. Based on the readily bifunctionalized alkynes, sulfonyl azides and Schiff bases, possible monomer combination ways are fully achieved to realize the diversity of multicomponent polymerization. The tolerance of 4-membered heterocycles to acid and base was improved by optimizing the ring electron density and confirmed by DFT calculation. The obtained polymers possessed distinguished properties such as good stability and stereoselectivity. The AIE characteristics inherited from the TPE moieties enabled the polymers to serve as potential bifunctional chemosensor for Pd^{2+} and $Cr_2O_7^{2-}$ detection. Simple prototype devices using P**1a**/**2a**/**3a** on solid support for daily detection was explored. In all, the feasible strategy used in this work will promote further research on multicomponent polymerization to construct and expand the small-membered heterocyclic polymers. It provides a useful guidance to manipulate the properties and functionalities of materials by appropriate structure design.

ASSOCIATED CONTENT

Supporting Information. The following files are available free of charge. Details of experimental section; effect of solvent and catalyst on the polymerization; characterization data (HRMS, FT-IR,

NMR, TGA and DSC); absorption spectra and emission spectra of model compounds and polymers (PDF). Crystal data of *trans*-**M** (CCDC: 2150052).

AUTHOR INFORMATION

Corresponding Author

*hanting@szu.edu.cn

*chjacky@ust.hk

*tangbenz@cuhk.edu.cn

Notes

The authors declare no competing financial interest.

ACKNOWLEDGMENT

We are grateful for financial support from the National Natural Science Foundation of China (21905176 and 21788102), the Science and Technology Plan of Shenzhen (JCYJ20160229205601482, JCYJ20170818113602462, JCYJ20180507183832744, and JCYJ20190808142403590), the Research Grants Council of Hong Kong (16304819, 16305320, N-HKUST609/19, and C6014-20W/16), and the Innovation and Technology Commission (ITC-CNERC14SC01).

REFERENCES

(1) Shonaike, G. O.; Advani, S. G. *Advanced Polymeric Materials: Structure Property Relationships*. CRC Press, 2003.

(2) Irmisch, P.; Ouldridge, T. E.; Seidel, R. Modeling DNA-Strand Displacement Reactions in the Presence of Base-Pair Mismatches. *J. Am. Chem. Soc.* **2020,** *142*, 11451-11463.

(3) Baird, D. G.; Collias, D. I. *Polymer Processing: Principles and Design*. John Wiley & Sons, 2014.

(4) Wang, Y.; Wang, Q.; Pan, X. Controlled Radical Polymerization toward Ultra-High Molecular Weight by Rationally Designed Borane Radical Initiators. *Cell Reports Physical Science* **2020,** *1*, 100073.

(5) Liu, X.; Han, T.; Lam, J. W.; Tang, B. Z. Functional Heterochain Polymers Constructed by Alkyne Multicomponent Polymerizations. *Macromol. Rapid Commun.* **2021,** *42*, 2000386.

(6) He, B.; Zhang, J.; Zhang, H.; Liu, Z.; Zou, H.; Hu, R.; Qin, A.; Kwok, R. T.; Lam, J. W.; Tang, B. Z. Catalyst-free Multicomponent Tandem Polymerizations of Alkyne and Amines toward Nontraditional Intrinsic Luminescent Poly(aminomaleimide)s. *Macromolecules* **2020,** *53*, 3756-3764.

(7) Kreye, O.; Toth, T.; Meier, M. A. Introducing Multicomponent Reactions to Polymer Science: Passerini Reactions of Renewable Monomers. *J. Am. Chem. Soc.* **2011,** *133*, 1790-1792.

(8) Deng, X. X.; Li, L.; Li, Z. L.; Lv, A.; Du, F. S.; Li, Z. C. Sequence Regulated Poly(ester-amide)s based on Passerini Reaction. *ACS Macro Lett.* **2012,** *1*, 1300-1303.

(9) Chan, C. Y.; Tseng, N.-W.; Lam, J. W.; Liu, J.; Kwok, R. T.; Tang, B. Z. Construction of Functional Macromolecules with Well-defined Structures by Indium-Catalyzed Three-component Polycoupling of Alkynes, Aldehydes, and Amines. *Macromolecules* **2013,** *46*, 3246-3256.

(10) Boukis, A. C.; Llevot, A.; Meier, M. A. High Glass Transition Temperature Renewable Polymers via Biginelli Multicomponent Polymerization. *Macromol. Rapid Commun.* **2016,** *37*, 643-649.

(11) Xue, H.; Zhao, Y.; Wu, H.; Wang, Z.; Yang, B.; Wei, Y.; Wang, Z.; Tao, L. Multicomponent Combinatorial Polymerization via the Biginelli Reaction. *J. Am. Chem. Soc.* **2016,** *138*, 8690-8693.

(12) Kim, H.; Bang, K. T.; Choi, I.; Lee, J. K.; Choi, T. L. Diversity-Oriented Polymerization: One-Shot Synthesis of Library of Graft and Dendronized Polymers by Cu-Catalyzed Multicomponent Polymerization. *J. Am. Chem. Soc.* **2016,** *138*, 8612-8622.

(13) Deng, H.; Han, T.; Zhao, E.; Kwok, R. T.; Lam, J. W.; Tang, B. Z. Multicomponent Click Polymerization: A Facile Strategy toward Fused Heterocyclic Polymers. *Macromolecules* **2016,** *49*, 5475-5483.

(14) Deng, H.; Han, T.; Zhao, E.; Kwok, R. T.; Lam, J. W.; Tang, B. Z. Multicomponent Polymerization: Development of a One-pot Synthetic Route to Functional Polymers Using Diyne, N-sulfonyl Azide and Water/Ethanol as Reactants. *Polym. Chem.* **2016,** *7*, 5646-5654.

(15) Xu, L.; Hu, R.; Tang, B. Z. Room Temperature Multicomponent Polymerizations of Alkynes, Sulfonyl Azides, and Iminophosphorane toward Heteroatom-rich Multifunctional Poly(phosphorus amidine)s. *Macromolecules* **2017,** *50*, 6043-6053.

(16) Xu, L.; Zhou, F.; Liao, M.; Hu, R.; Tang, B. Z. Room Temperature Multicomponent Polymerizations of Alkynes, Sulfonyl Azides, and N-protected Isatins toward Oxindole-Containing Poly(N-acylsulfonamide)s. *Polym. Chem.* **2018,** *9*, 1674-1683.

(17) Xu, L.; Hu, R.; Tang, B. Z. Room Temperature Multicomponent Polymerizations of Alkynes, Sulfonyl Azides, and Iminophosphorane toward Heteroatom-Rich Multifunctional Poly(phosphorus amidine)s. *Macromolecules* **2017,** *50*, 6043-6053.

(18) Zheng, C.; Deng, H.; Zhao, Z.; Qin, A.; Hu, R.; Tang, B. Z. Multicomponent Tandem Reactions and Polymerizations of Alkynes, Carbonyl Chlorides, and Thiols. *Macromolecules* **2015,** *48*, 1941-1951.

(19) Deng, H.; Hu, R.; Zhao, E.; Chan, C. Y.; Lam, J. W.; Tang, B. Z. One-pot Three-component Tandem Polymerization toward Functional Poly(arylene thiophenylene) with Aggregation-enhanced Emission Characteristics. *Macromolecules* **2014,** *47*, 4920-4929.

(20) Deng, H. Q.; He, Z. K.; Lam, J. W. Y.; Tang, B. Z. Regio- and Stereoselective Construction of Stimuli-responsive Macromolecules by a Sequential Coupling-Hydroamination Polymerization Route. *Polym. Chem.* **2015,** *6*, 8297-8305.

(21) Deng, H.; Hu, R.; Leung, A. C.; Zhao, E.; Lam, J. W.; Tang, B. Z. Construction of Regio- and Stereoregular Poly(enaminone)s by Multicomponent Tandem Polymerizations of Diynes, Diaroyl Chloride and Primary Amines. *Polym. Chem.* **2015,** *6*, 4436-4446.

(22) Deng, H.; Zhao, E.; Leung, A. C.; Hu, R.; Zhang, Y.; Lam, J. W.; Tang, B. Z. Multicomponent Sequential Polymerizations of Alkynes, Carbonyl Chloride and Amino Ester Salts toward Helical and Luminescent Polymers. *Polym. Chem.* **2016,** *7*, 1836-1846.

(23) Tang, X.; Zhang, L.; Hu, R.; Tang, B. Z. Multicomponent Tandem Polymerization of Aromatic Alkynes, Carbonyl Chloride, and Fischer's Base toward Poly(diene merocyanine)s. *Chin. J. Chem.* **2019,** *37*, 1264-1270.

(24) Han, T.; Deng, H.; Qiu, Z.; Zhao, Z.; Zhang, H.; Zou, H.; Leung, N. L.; Shan, G.; Elsegood, M. R.; Lam, J. W. Y. Lam, and Tang, B. Z. Facile Multicomponent Polymerizations toward Unconventional Luminescent Polymers with Readily Openable Small Heterocycles. *J. Am. Chem. Soc.* **2018,** *140*, 5588-5598.

(25) Sillion, B. Aromatic and Heterocyclic Polymers - What Future? *High Perform. Polym.* **1999,** *11*, 417-436.

(26) Deng, H.; Han, T.; Zhao, E.; Kwok, R. T. K.; Lam, J. W. Y.; Tang, B. Z. Multicomponent Click Polymerization: A Facile Strategy toward Fused Heterocyclic Polymers. *Macromolecules* **2016,** *49*, 5475-5483.

(27) Tang, X.; Zheng, C.; Chen, Y.; Zhao, Z.; Qin, A.; Hu, R.; Tang, B. Z. Multicomponent Tandem Polymerizations of Aromatic Diynes, Terephthaloyl Chloride, and Hydrazines toward Functional Conjugated Polypyrazoles. *Macromolecules* **2016,** *49*, 9291-9300.

(28) Wu, Y.; He, B.; Quan, C.; Zheng, C.; Deng, H.; Hu, R.; Zhao, Z.; Huang, F.; Qin, A.; Tang, B. Z. Metal-Free Poly-Cycloaddition of Activated Azide and Alkynes toward Multifunctional Polytriazoles: Aggregation-Induced Emission, Explosive Detection, Fluorescent Patterning, and Light Refraction. *Macromol. Rapid Commun.* **2017,** *38*, 1700070.

(29) Song, B.; Hu, K.; Qin, A.; Tang, B. Z. Oxygen as a Crucial Comonomer in Alkyne-based Polymerization toward Functional Poly(tetrasubstituted furan)s. *Macromolecules* **2018,** *51*, 7013-7018.

(30) Wei, B.; Li, W.; Zhao, Z.; Qin, A.; Hu, R.; Tang, B. Z. Metal-free Multicomponent Tandem Polymerizations of Alkynes, Amines, and Formaldehyde toward Structure-and Sequence-Controlled Luminescent Polyheterocycles. *J. Am. Chem. Soc.* **2017,** *139*, 5075-5084.

(31) Han, T., *Syntheses of Functional Polymers by New Alkyne-Based Polymerizations*. Hong Kong University of Science and Technology (Hong Kong), 2019.

(32) Whiting, M.; Fokin, V. Copper-Catalyzed Reaction Cascade: Direct Conversion of Alkynes into N-Sulfonylazetidin-2-Imines. Angew. Chem. Int. Ed. **2006**, *45*, 3157-3161.

(33) Xu, L.; Zhou, T.; Liao, M.; Hu, R.; Tang, B. Z. Multicomponent Polymerizations of Alkynes, Sulfonyl Azides, and 2-Hydroxybenzonitrile/2-Aminobenzonitrile toward Multifunctional

Iminocoumarin/Quinoline-Containing Poly (N-sulfonylimine)s. ACS Macro Lett. **2019,** *8*, 101-106.

(34) Liu, Y.; Wang, J.; Huang, D.; Zhang, J.; Guo, S.; Hu, R.; Zhao, Z.; Qin, A.; Tang, B. Z. Synthesis of 1,5-Regioregular Polytriazoles by Efficient NMe4OH-Mediated Azide–Alkyne Click Polymerization. *Polym. Chem.* **2015,** *6*, 5545-5549.

(35) Han, T.; Zhao, Z.; Lam, J. W. Y.; Tang, B. Z. Monomer Stoichiometry Imbalance-Promoted Formation of Multisubstituted Polynaphthalenes by Palladium-Catalyzed Polycouplings of Aryl Iodides and Internal Diynes. *Polym. Chem.* **2018,** *9*, 885-893.

(36) McMurry, J. E., *Fundamentals of Organic Chemistry*. Cengage Learning, 2010.

(37) Han, T.; Deng, H.; Chris, Y.; Gui, C.; Song, Z.; Kwok, R. T.; Lam, J. W.; Tang, B. Z. Functional Isocoumarin-Containing Polymers Synthesized by Rhodium-catalyzed Oxidative Polycoupling of Aryl Diacid and Internal Diyne. *Polym. Chem.* **2016,** *7*, 2501-2510.

(38) Xingpeng, C.; Jiaxi, X. Regioselective Ring-Opening Reactions of Unsymmetric Azetidines. *Prog. Chem.* **2017,** *29*, 181.

(39) Lu, T.; Chen, F. W. Multiwfn: A Multifunctional Wavefunction Analyzer. *J. Comput. Chem.* **2012,** *33*, 580-592.

(40) Roy, R. K.; Krishnamurti, S.; Geerlings, P.; Pal, S. Local Softness and Hardness Based Reactivity Descriptors for Predicting Intra- and Intermolecular Reactivity Sequences: Carbonyl Compounds. *J. Phys. Chem. A* **1998,** *102*, 3746-3755.

(41) Lu, T.; Chen, F. Quantitative Analysis of Molecular Surface Based on Improved Marching Tetrahedra Algorithm. *J. Mol. Graph. Model.* **2012,** *38*, 314-323.

(42) Fukui, K. Role of Frontier Orbitals in Chemical Reactions. *Science* **1982,** *218*, 747-754.

(43) Parr, R. G.; Yang, W. Density Functional Approach to the Frontier-Electron Theory of Chemical Reactivity. *J. Am. Chem. Soc.* **1984,** *106*, 4049-4050.

(44) Morell, C.; Grand, A.; Toro-Labbe, A. New Dual Descriptor for Chemical Reactivity. *J. Phys. Chem. A* **2005,** *109*, 205-212.

(45) Han, T.; Yan, D.; Wu, Q.; Song, N.; Zhang, H.; Wang, D. Aggregation-Induced Emission: A Rising Star in Chemistry and Materials Science. *Chinese J. Chem.* **2021,** *39*, 677-689.

(46) Luo, J.; Xie, Z.; Lam, J. W.; Cheng, L.; Chen, H.; Qiu, C.; Kwok, H. S.; Zhan, X.; Liu, Y.; Zhu, D.; Tang, B. Z. Aggregation-Induced Emission of 1-Methyl-1,2,3,4,5-Pentaphenylsilole. *Chem. Commun.* **2001**, 1740-1741.

(47) Han, T.; Liu, L.; Wang, D.; Yang, J.; Tang, B. Z. Mechanochromic Fluorescent Polymers Enabled by AIE Processes. *Macromol. Rapid Commun.* **2021,** *42*, 2000311.

(48) Gao, Q.; Xiong, L. H.; Han, T.; Qiu, Z.; He, X.; Sung, H. H. Y.; Kwok, R. T. K.; Williams, I. D.; Lam, J. W. Y.; Tang, B. Z. Three-Component Regio- and Stereoselective Polymerizations toward Functional Chalcogen-Rich Polymers with AIE-Activities. *J. Am. Chem. Soc.* **2019,** *141*, 14712-14719.

(49) Mei, J.; Leung, N. L.; Kwok, R. T.; Lam, J. W.; Tang, B. Z. Aggregation-Induced Emission: Together We Shine, United We Soar! *Chem. Rev.* **2015,** *115*, 11718-11940.

(50) Kielhorn, J.; Melber, C.; Keller, D.; Mangelsdorf, I. Palladium–A Review of Exposure and Effects to Human Health. *Int. J. Hyg. Environ. Health* **2002,** *205*, 417-432.

(51) Brasili, E.; Bavasso, I.; Petruccelli, V.; Vilardi, G.; Valletta, A.; Dal Bosco, C.; Gentili, A.; Pasqua, G.; Di Palma, L. Remediation of Hexavalent Chromium Contaminated Water through Zero-Valent Iron Nanoparticles and Effects on Tomato Plant Growth Performance. *Sci. Rep.* **2020,** *10*, 1-11.

(52) Uddin, M. N.; Desai, F.; Asmatulu, E. Engineered Nanomaterials in the Environment: Bioaccumulation, Biomagnification and Biotransformation. *Environ. Chem. Lett.* **2020,** *18*, 1073-1083.

(53) Han, T.; Wang, X.; Wang, D.; Tang, B. Z. Functional Polymer Systems with Aggregation-Induced Emission and Stimuli Responses. *Top. Curr. Chem.* **2021,** *379*, 7.

(54) Alam, P.; Leung, N. L. C.; Zhang, J.; Kwok, R. T. K.; Lam, J. W. Y.; Tang, B. Z. AIE-based Luminescence Probes for Metal Ion Detection. *Coord. Chem. Rev.* **2021,** *429*, 213693.

(55) Liu, J.; Zhong, Y.; Lu, P.; Hong, Y.; Lam, J. W.; Faisal, M.; Yu, Y.; Wong, K. S.; Tang, B. Z. A Superamplification Effect in the Detection of Explosives by a Fluorescent Hyperbranched Poly(silylenephenylene) with Aggregation-Enhanced Emission Characteristics. *Polym. Chem.* **2010,** *1*, 426-429.

(56) He, B.; Su, H.; Bai, T.; Wu, Y.; Li, S.; Gao, M.; Hu, R.; Zhao, Z.; Qin, A.; Ling, J. Spontaneous Amino-yne Click Polymerization: A Powerful Tool toward Regio-and Stereospecific Poly(β-aminoacrylate)s. *J. Am. Chem. Soc.* **2017,** *139*, 5437-5443.

(57) Gao, M.; Lam, J. W. Y.; Liu, Y.; Li, J.; Tang, B. Z. A New Route to Functional Polymers: Atom-economical Synthesis of Poly(pyrazolylnaphthalene)s by Rhodium-Catalyzed Oxidative Polycoupling of Phenylpyrazole and Internal Diynes. *Polym. Chem.* **2013,** *4*, 2841-2849.

(58) Gao, M.; Lam, J. W. Y.; Li, J.; Chan, C. Y. K.; Chen, Y.; Zhao, N.; Han, T.; Tang, B. Z. Stoichiometric Imbalance-Promoted Synthesis of Polymers Containing Highly Substituted Naphthalenes: Rhodium-Catalyzed Oxidative Polycoupling of Arylboronic Acids and Internal Diynes. *Polym. Chem.* **2013,** *4*, 1372-1380.

(59) Liu, Y.; Roose, J.; Lam, J. W. Y.; Tang, B. Z. Multicomponent Polycoupling of Internal Diynes, Aryl Diiodides, and Boronic Acids to Functional Poly(tetraarylethene)s. *Macromolecules* **2015,** *48*, 8098-8107.